Na^+/H^+ Antiporter from *Synechocystis* Species PCC 6803, Homologous to SOS1, Contains an Aspartic Residue and Long C-Terminal Tail Important for the Carrier Activity

Akira Hamada, Takashi Hibino, Tatsunosuke Nakamura, and Teruhiro Takabe*

Research Institute of Meijo University, Tenpaku-ku, Nagoya, Aichi 468–8502, Japan (A.H., T.T.); Department of Chemistry, Faculty of Science and Technology, Meijo University, Tenpaku-ku, Nagoya, Aichi 468–8502, Japan (T.H., T.T.); and Laboratory of Membrane Biochemistry, Faculty of Pharmaceutical Science, Chiba University, Inage-ku, Chiba 263–8522, Japan (T.N.)

A putative Na^+/H^+ antiporter gene whose deduced amino acid sequence was highly homologous to the NhaP antiporter from *Pseudomonas aeruginosa* and SOS1 antiporter from Arabidopsis was isolated from *Synechocystis* sp. PCC 6803. The *Synechocystis* NhaP antiporter (SynNhaP) was expressed in *Escherichia coli* mutant cells, which were deficient in Na^+/H^+ antiporters. It was found that the SynNhaP complemented the salt-sensitive phenotype of the *E. coli* mutant. Membrane vesicles prepared from the *E. coli* mutant transformed with the SynNhaP exhibited the Na^+/H^+ and Li^+/H^+ antiporter activities, and their activities were insensitive to amiloride. Moreover, its activity was very high between pH 5 and 9. The replacement of aspartate-138 in SynNhaP with glutamate or tyrosine inactivated the SynNhaP antiporter activity. The deletion of a part of the long C-terminal hydrophilic tail significantly inhibited the antiporter activity. A topological model suggests that aspartate-138 in SynNhaP is conserved in NhaP, SOS1, and AtNHX1 and is involved in the exchange activity. Thus, it appeared that the SynNhaP would provide a model system for the study of structural and functional properties of eucaryotic Na^+/H^+ antiporters.

The Na^+/H^+ antiporters catalyze the exchange of Na^+ for H^+ across membranes and play a variety of functions such as the regulation of internal pH, cell volume, and sodium level in the cytoplasm (Padan and Schuldiner, 1996). In *Escherichia coli*, three antiporters (NhaA, NhaB, and ChaA) are known, and their functional characteristics have been well described (Padan and Schuldiner, 1996). In yeast, the Na^+/H^+ antiporters localized in the prevacuole membrane (NHX1) (Nass et al., 1997; Nass and Rao, 1998) and the plasma membrane (SOD2) (Jia et al., 1992; Hahnenberger et al., 1996) have been reported. In animals, six kinds of Na^+/H^+ antiporters (exchangers) (NHE1-6) have been found (Orlowski and Grinstein, 1997); the mitochondrial localization was demonstrated in NHE6 (Numata et al., 1998). A new unique Na^+/H^+ antiporter (NhaP), which has no homology to NhaA, NhaB, and ChaA, has been found recently in *Pseudomonas aeruginosa* (Utsugi et al., 1998).

In plants, Na^+/H^+ antiporters, homologous to the vacuole localized NHX1, have been isolated from Arabidopsis (AtNHX1) (Gaxiola et al., 1999) and *Oryza sativa* (Fukuda et al., 1999). The enhanced salt tolerance of Arabidopsis has been demonstrated by the overexpression of AtNHX1 (Apse et al., 1999). The SOS1 gene, which is essential for Na^+ and K^+ homeostasis, recently was isolated from Arabidopsis (Shi et al., 2000). The expression of SOS1 was significantly enhanced by NaCl stress, especially in the root. SOS1 exhibited very high sequence homology to the NhaP antiporter from *P. aeruginosa* (Utsugi et al., 1998), but is more distantly related to a cluster of organellar Na^+/H^+ antiporters such as AtNHX1, NHX1, or NHE6 (Shi et al., 2000). From these results, they suggested that the SOS1 is localized in the plasma membranes (Shi et al., 2000).

From the complete nucleotide sequence of a cyanobacterium *Synechocystis* sp. 6803, it was suggested that the *Synechocystis* sp. 6803 contains at least five Na^+/H^+ antiporter genes (Kaneko et al., 1996). However, their functional characterization has never been reported. During the homology search, we found that two genes (*synnha*P and *synnha*P2) are highly homologous to the NhaP from *P. aeruginosa*. Moreover, it was suggested that the Asp-138 in SynNhaP is conserved in eucaryotic Na^+/H^+ exchangers and the C-terminal hydrophilic tail in SynNhaP is much longer than that of the NhaP. Therefore, we isolated one of two *nha*P genes whose deduced amino acid sequence is more homologous to NhaP and SOS1. We constructed the Asp-138 mutants as well as the C-terminal deleted mutant and expressed it in the *E.*

[1] This work was supported in part by the Grants-in-Aid for Scientific Research from the Ministry of Education, Science and Culture of Japan, the High-Tech Research Center of Meijo University, and the Program for Promotion of Basic Research Activities for Innovative Biosciences (PROBRAIN) of the Japanese Ministry of Agriculture, Forestry and Fisheries.

* Corresponding author; e-mail takabe@meijo-u.ac.jp; fax 81–52–832–1545.

coli TO114 cells in which *nha*A, *nha*B, and *cha*A genes were deleted (Ohyama et al., 1994; Enomoto et al., 1998). SynNhaP complemented the salt-sensitive phenotype of the *E. coli* mutants and its Asp-138 and C-terminal tail are important for the Na^+/H^+ antiporter activity.

RESULTS

Isolation of SynNhaP Gene

The homology search revealed that *Synechocystis* sp. PCC 6803 did not contain the genes homologous to the *nha*A, *nha*B, and *cha*A from *E. coli*. In contrast, two genes (accession nos. D90910 and D90914) homologous to *nha*P from *P. aeruginosa* were found. The former gene encodes a polypeptide of 527 amino acid residues (SynNhaP), whereas the latter one encodes a polypeptide of 540 amino acid residues (SynNhaP2) as shown in Figure 1A. Two deduced proteins showed high homology to NhaP from *P. aeruginosa* (approximately 33%–34% identity in amino acids), and SOS1 from Arabidopsis (31%–34%) in the corresponding regions, but slightly lower similarities to the human NHE1 (29%–30%) and the organellar Na^+/H^+ antiporters such as AtNHX1 and NHE6 (28%–30%). Because the deduced amino acid sequence of SynNhaP showed higher similarities to SOS1 and NhaP than that of SynNhaP2 (Fig. 1, A and B), we examined the isolation of *synnha*P gene from *Synechocystis* sp. PCC 6803 by the PCR technique. The nucleotide sequence of the isolated gene completely coincided with that reported (Kaneko et al., 1996). As shown in Figure 1A, the Asp-138 in SynNhaP was conserved in all eucaryotic type Na^+/H^+ exchangers (SOS1, AtNHX1, NHE1, and NHX1) examined as well as NhaP. In addition, the SynNhaP contained a longer hydrophilic C-terminal tail than NhaP from *P. aeruginosa*.

Expression of Wild-Type and Mutant SynNhaP Antiporters in *E. coli*

As described in "Materials and Methods," the isolated synnhaP gene was ligated into the pTrc-His2C plasmid. The resulting plasmid, pSNhaP, encodes the SynNhaP fused in frame to six histidines. The D138E, D138Y, and C-terminal deleted mutants were expressed by using the plasmids, pSNhaPD138E, pSNhaPD138Y, and pSNhaPΔC, all of which retained the His tag. Due to the absence of Na^+/H^+ antiporter genes (*nha*A, *nha*B, and *cha*A) in *E. coli* host cells (TO114), the host cell itself could not grow in the presence of 0.2 M NaCl at pH 8.

To examine whether the SynNhaP catalyzes the exchange between Na^+ and H^+ across membranes, the *E. coli* TO114 cells were transformed with pTrc-His2C, pSNhaP, pSNhaPD138E, pSNhaPD138Y, and pSNhaPΔC. After expression of these genes, the membrane fractions were isolated and subjected to SDS-PAGE and immunoblotting analysis with the antibody raised against the 6×-His tag. The *E. coli* cells transformed with pSNhaP, pSNhaPD138E, and pSNhaPD138Y exhibited a single cross-reaction band corresponding to approximately 53 kD (Fig. 2). As expected from its shorter C-terminal tail, the pSNhaPΔC mutant migrated faster than other SynNhaP antiporters. The *E. coli* cells transformed with the vector alone did not show any cross-reaction band. The accumulation levels of wild-type and mutant SynNhaP were similar as shown in Figure 2. These results indicate that both the SynNhaP and its mutants could be expressed and assembled in *E. coli* membranes.

Complementation of Salt-Sensitive *E. coli* Cells

Figure 3 shows the growth curves of *E. coli* TO114 cells transformed with pTrc-His2C, pSNhaP, pSNhaPD138E, pSNhaPD138Y, and pSNhaPΔC. All these *E. coli* cells showed similar growth rates in LBK medium, in which NaCl in the original L broth was replaced by KCL (87mM), at pH 7.0 (Fig. 3A). However, the *E. coli* cells transformed with pTrc-His2C, pSNhaPD138E, and pSNhaPD138Y could not grow during the 24-h incubation in the presence of NaCl at 200 mM or higher concentration in LBK medium (Fig. 3, B and D). In contrast, the *E. coli* cells transformed with pSNhaP and pSNhaPΔC could grow even in the presence of 200 mM NaCl, although their growth rates were decreased with increasing concentrations of NaCl (Fig. 3, B and D). *E. coli* cells transformed with pSNhaPΔC showed lower growth rates than the cells transformed with pSNhaP. These results indicate that the His-tagged SynNhaP could function as Na^+/H^+ antiporter in *E. coli* cells and the replacement of Asp-138 with Glu or Tyr abolished the complementation ability of SynNhaP. The deletion of hydrophilic C-terminal 56 amino acid residues partially inhibited the complementation ability of SynNhaP.

Similar results were obtained for the SynNhaP, SynNhaPD138E, and SynNhaPD138Y grown in the LBK medium containing LiCl as shown in Figures 3, C and E. However, different effects were observed in SynNhaPΔC. As shown in Figure 3E, SynNhaPΔC could not complement the LiCl-sensitive phenotype of *E. coli* mutant during the 11-h incubation in the presence of 4 mM LiCl. However, the *E. coli* cells transformed with pSNhaPΔC started to grow after 24 h of incubation (Fig. 3E).

Essentially similar results were obtained when the growth medium was pH 8.0, although a lower salt concentration must be used due to the increased sensitivity of *E. coli* mutant to salt at an alkaline pH (Ohyama et al., 1994). These results suggest that SynNhaP could catalyze the exchanges between Na^+ and H^+ and also between Li^+ and H^+, that Asp-138 is essential for the antiporter activity, and that the hydrophilic C-terminal 56 amino acid residues are

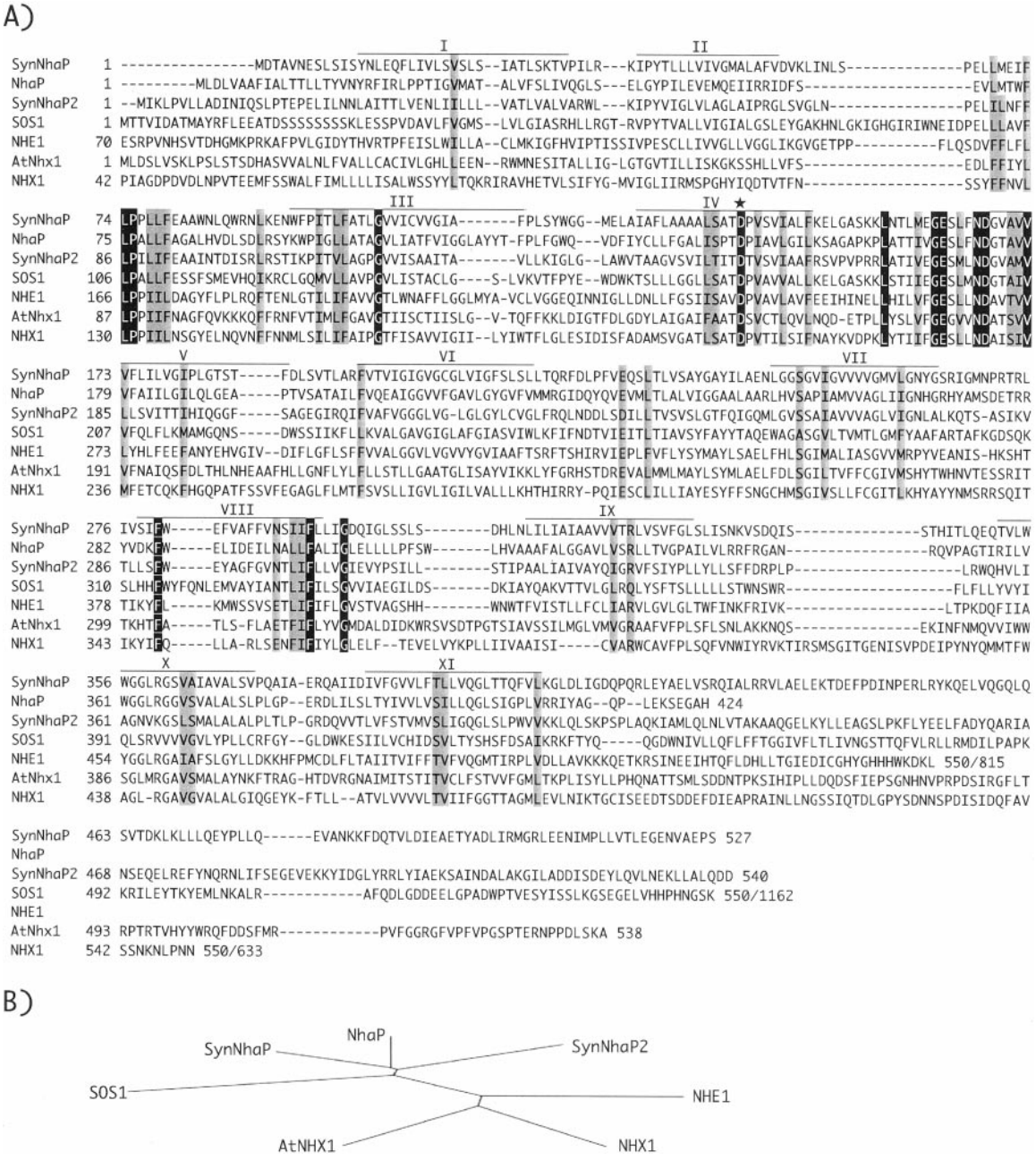

Figure 1. A, Alignment of the deduced amino acid sequences of Na^+/H^+ antiporters from seven organisms. The sequences were aligned by the program ClustalW. The alignment is based on the N-terminal 550 amino acid residues in the cases of SOS1, human NHE1, and yeast NHX1. The amino acid residues conserved in all sequences are highlighted in black and conservative substitutions are shown in gray. The conserved Asp (Asp-138 in SynNhaP) is shown by an asterisk. Predicted membrane spanning regions were marked above the alignment. B, Phylogenetic analysis of seven Na^+/H^+ antiporters. Multiple sequence alignment and generation of phylogenetic tree were performed with ClustalW and TreeView software, respectively.

important for LiCl tolerance but have minor effects on NaCl tolerance.

Na^+/H^+ Antiporter Activity in the Everted Membrane Vesicles

To examine directly the antiporter activity of wild-type and mutant SynNhaP, the everted membrane vesicles were prepared and their antiporter activities were monitored by measuring the dequenching of acridine orange fluorescence upon addition of NaCl or LiCl. As shown in Figure 4A, the dequenching of fluorescence was observed upon the addition of NaCl in the SynNhaP-expressing cells, but not in the control (pTrc-His2C) cells, indicating that SynNhaP has Na^+/H^+ antiporter activity. Figures 4, B and C

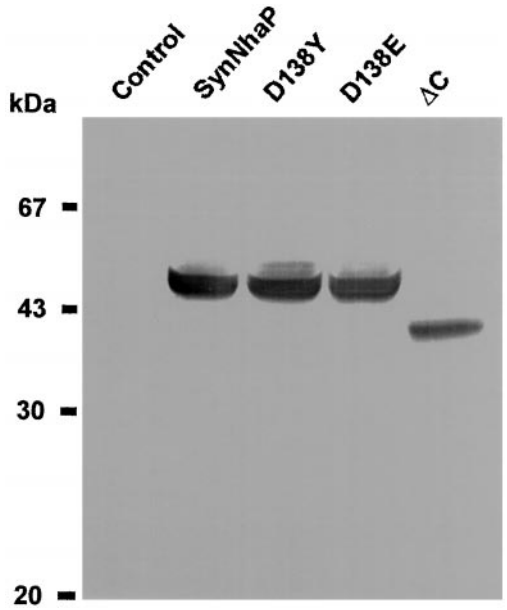

Figure 2. Immunoblotting analyses of five kinds of Na^+/H^+ antiporters. The membrane fractions of *E. coli* were prepared. Equal amounts of proteins (20 μg) were applied on SDS-PAGE and visualized by using the antibodies raised against 6×-His tag. The plasmids used for the transformation of *E. coli* were follows: lane 1, pTrc-His2C; lane 2, pSynNhaP; lane 3, pSNhaPD138Y; lane 4, pSNhaPD138E; lane 5, pSNhaPΔC. Numerals on the left indicate molecular mass.

show that Li^+ could be replaced with Na^+, whereas K^+ or Ca^{2+} or Mg^{2+} could not. It is known that amiloride inhibits the activity of Na^+/H^+ antiporters from animals (Orlowski, 1993), plants (Blumwald et al., 1987), and some bacteria (Pinner et al., 1995). Figure 4D shows the effects of amiloride on the activities of SynNhaP. SynNhaP was insensitive to amiloride both in Na^+/H^+ and Li^+/H^+ exchange activities.

Na^+/H^+ Antiporter Activity of SynNhaP Mutants

Figure 4B shows that the replacement of Asp-138 with Glu-138 or Tyr-138 abolished the Na^+/H^+ and Li^+/H^+ exchange activities of SynNhaP, indicating the importance of Asp-138 for the antiporter activity of SynNhaP.

Figure 4B also shows that SynNhaPΔC had very low Na^+/H^+ and Li^+/H^+ antiporter activities. This low activity presumably partially complemented the NaCl-sensitive phenotype of the *E. coli* mutants but not the LiCl-sensitive phenotype.

Effects of pH on the Na^+/H^+ Antiporter Activity

Next, we examined the effects of pH on the antiporter activity of the SynNhaP. Although the respiration-driven fluorescence quenching of acridine orange was decreased when the reaction mixture was made acidic (pH 5), the fluorescence dequenching upon addition of NaCl occurred to an extent similar to that obtained at pH 7.0. Upon addition of NH_4Cl, the fluorescence intensity recovered almost to the original level (data not shown). Thus, it appeared that the SynNhaP has high Na^+/H^+ antiporter activities at an acidic pH (pH 5) as shown in Figure 5. Essentially similar results were obtained at an alkaline pH of 9, indicating that the SynNhaP had very high Na^+/H^+ antiporter activities over a wide range of pH between 5 and 9, which is quite different from those of *E. coli* NhaA. In *E. coli* NhaA, the antiporter activity could not be observed below pH 7.5, whereas the activity increased with increasing pH (Padan and Schuldiner, 1996). The SynNhaP exhibited similar pH dependences for the Na^+/H^+ and Li^+/H^+ exchange activities (Fig. 5).

The SynNhaPD138E and SynNhaPD138Y mutants had no Na^+/H^+ and Li^+/H^+ exchange activities at pH values lower than 8.0, but they showed small activities at an alkaline pH as shown in Figure 5.

Topological Model for SynNhaP

From the analysis of the hydropathy plot (Kyte and Doolittle, 1982) and the transmembrane (TM) prediction program (Hofmann and Stoffel, 1992) of the SynNhaP sequence, we predicted that the SynNhaP has 11 putative transmembrane segments (Fig. 6). The amino acid sequence of SynNhaP shows that it has 49 negative and 34 positive charges. Among them, three negative and two positive charges were located in hydrophobic segments, and only the Asp-138 was conserved in SynNhaP, NhaP, SOS1, AtNHX1, OsNHX1, NHX1, and mammalian NHE1. In this model, 28 negative and 23 positive charges were located in the cytoplasmic and 18 negative and nine positive charges were located in the periplasmic face of the membrane. Although the model is consistent with the so-called "positive inside rule" (von Heijne and Gavel, 1988) and the recently proposd one for human NHE1 (Wakabayashi et al., 2000), this is a tentative one and further study is required to obtain the insight on the structure of membrane spanning domains. Nevertheless, this model together with the experimental results presented in the above suggest that Asp-138 is involved in the exchange between Na^+ and H^+.

DISCUSSION

The data presented above clearly indicate that a putative eucaryotic type antiporter SynNhaP from *Synechocystis* sp. PCC 6803 had exchange activities between Na^+ and H^+ as well as Li^+ and H^+. This conclusion was based on the finding that the antiporter-deficient *E. coli* TO114 mutant cells became salt-tolerant by transformation with its gene and also by the direct observation of Na^+/H^+ as well as Li^+/H^+ antiporter activities in the transformant membrane vesicles. The most striking functional feature of

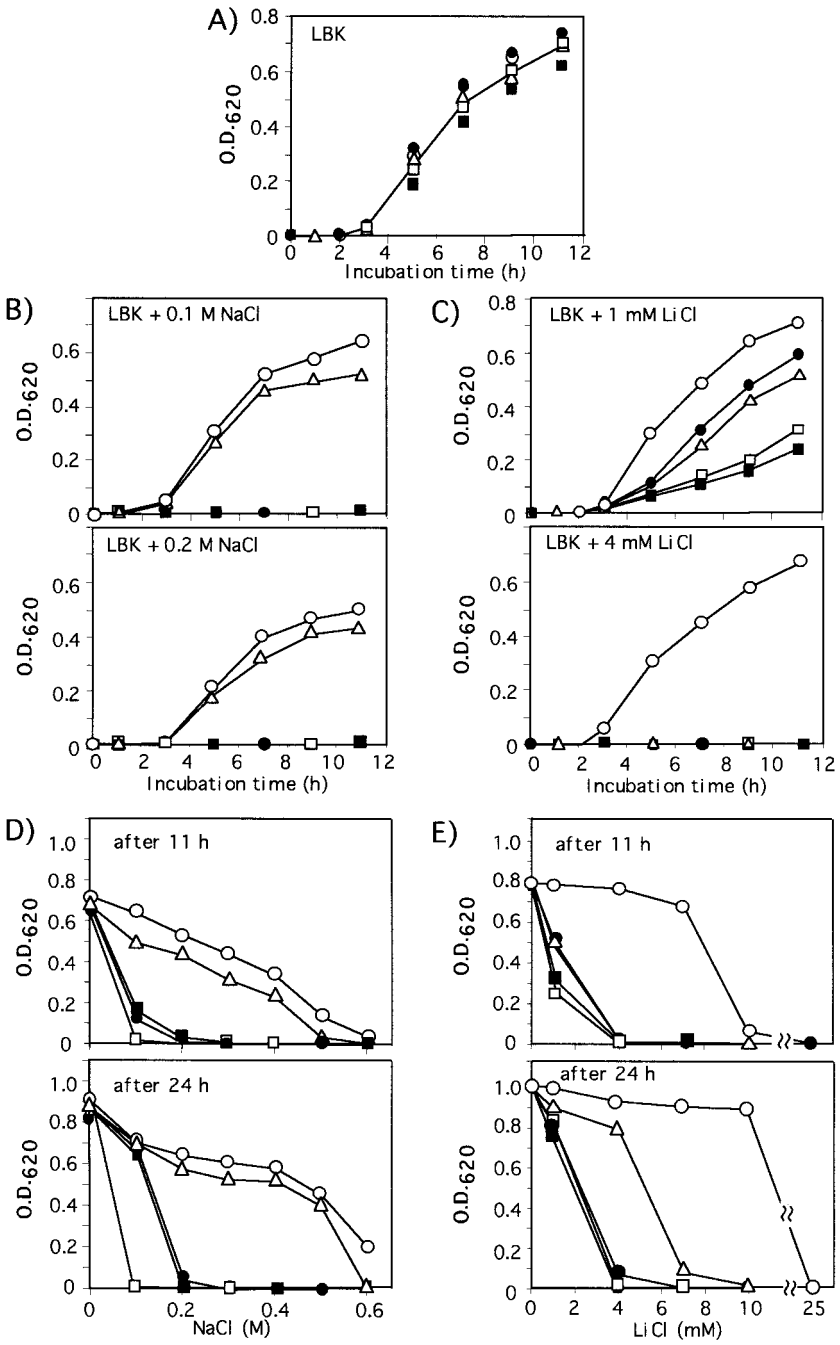

Figure 3. Effects of NaCl and LiCl on the growth rates of various kinds of *E. coli* cells. The control and transformant cells at logarithmic phase in LBK medium were subjected to salt stress by inoculation into fresh LBK medium containing indicated concentrations of NaCl or LiCl. A, Time courses of growth in LBK medium. B, Time courses of growth in LBK containing 0.1 or 0.2 M NaCl. C, Time courses of growth in LBK containing 1 or 4 mM LiCl. D, Growth after 11 or 24 h incubation with various kinds of concentrations of NaCl. E, Growth after 11 or 24 h incubation with LiCl of various concentrations. ●, Control cells; ○, SynNhaP-expressing cells; ■, SynNhaPD138E-expressing cells; □, SynNhaPD138Y-expressing cells; △, SynNhaPΔC-expressing cells. Each value shows the average of three independent measurements (SE was within 15%).

SynNhaP is that its activity was observed over a wide pH range between pH 5 and 9. In addition, it was shown that the Asp-138 in SynNhaP was essential for the exchange between Na^+ or Li^+ with H^+.

To date, only a few functional residues have been identified in antiporter proteins. Nothing is known about the NhaP antiporter. Although the importance of amino acid residues involving the amiloride-binding domain and glycosylation site have been reported in the mammalian NHE exchanger (Orlowski, 1993; Orlowski and Grinstein, 1997), the importance of Asp in the hydrophobic region has not been reported in eucaryotic Na^+/H^+ antiporters. Figure 1A suggests that the Asp-138 in SynNhaP corresponds to the Asp-238 in NHE1, but the mutagenesis study of Asp-238 in NHE1 has not been reported. In NhaA, the importance of Asp-133, -163, and -164 in the hydrophobic TM segments has been demonstrated (Nakamura et al., 1994; Inoue et al., 1995; Nakamura et al., 1995). Consistent with essentially no homology between SynNhaP and NhaA, the SynNhaP contains only one Asp in the hydrophobic TM segments. However, the local homology in the vicinity of Asp-138 in the SynNhaP and Asp-133 in

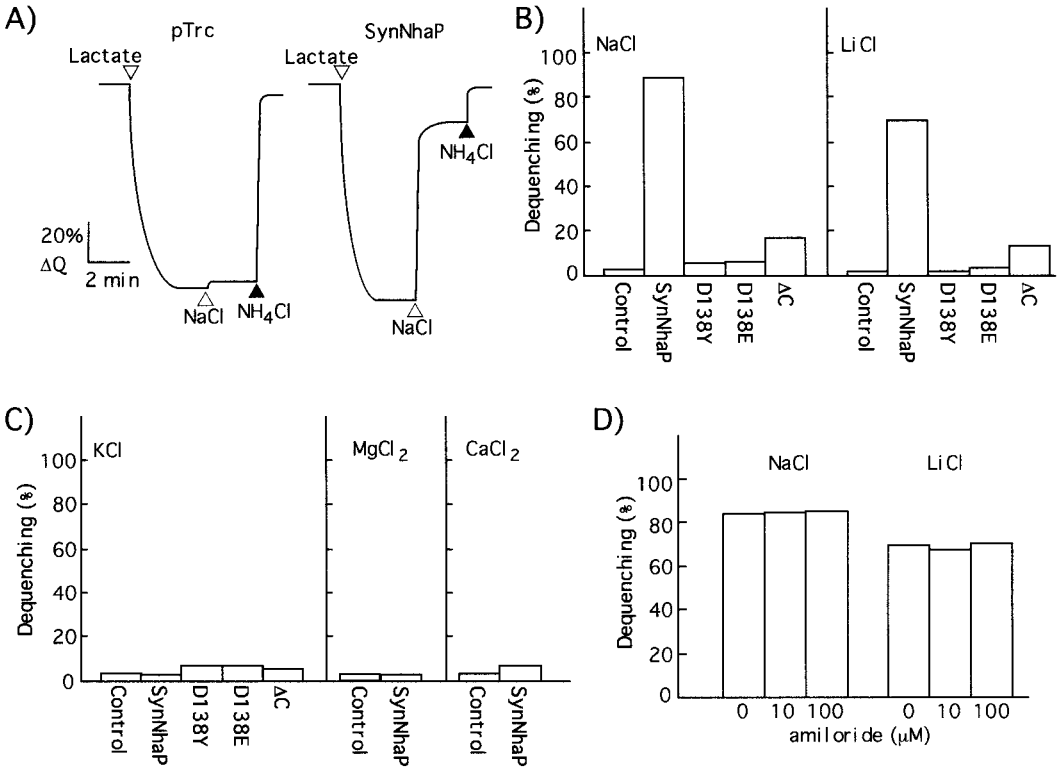

Figure 4. Na^+/H^+ antiporter activity measured by the acridine orange fluorescence quenching method. The control *E. coli* cells and *E. coli* cells expressing SynNhaP, SynNhaPD138E, SynNhaPD138Y, and SynNhaPΔC were grown in LBK medium without addition of extra salts. From these cells the everted membrane vesicles were prepared. A, Typical fluorescence traces. At the time indicated by downward arrows, Tris-lactate (final concentration 2 mM) was added to initiate the respiration induced fluorescence quenching. Then at the time indicated by upward arrows, salts (NaCl, LiCl, KCl, $CaCl_2$, $MgCl_2$) were added. The final salt concentration was 5 mM. Then NH_4^+ (final concentration 25 mM) was added to the assay mixture. The assay mixture was pH 8.0. The dequenching (%) was calculated from the ratio of NaCl-induced dequenching/lactate-induced quenching. B, NaCl- or LiCl-induced dequenching (%). C, KCl-, $MgCl_2$-, or $CaCl_2$-induced dequenching (%). D, Effects of amiloride on the NaCl- or LiCl-induced dequenching. Each value shows the average of three independent measurements (SE was within 8%).

NhaA has been suggested. This and the present data imply that Asp-138 might be involved in the exchange of cations, which must be verified experimentally. The present data also indicate that the replacement of Asp-138 with Glu abolished the Na^+/H^+ exchange activity. This suggests that the negative charge on Asp-138 is not sufficient for the exchange activity and the geometry in the vicinity of Asp-138 plays an important role.

It has been reported that NhaP from *P. aeruginosa* (Utsugi et al., 1998) has very low activity of exchange between Li^+ and H^+. Therefore, NhaP from *P. aeruginosa* could not complement the LiCl sensitivity of *E. coli* TO114 mutant cells although NhaA, NhaB, and NhaD could (Utsugi et al., 1998). These properties of NhaP are different from those observed in SynNhaP. The Li^+/H^+ antiporter activity of SynNhaP was almost the same as that of Na^+/H^+ antiporter (Figs. 4 and 5) and SynNhaP could confer the resistance not only to NaCl but also to LiCl stress (Fig. 3). At the present time, the molecular mechanisms for the different ion specificity between SynNhaP and NhaP remain to be clarified.

The different pH dependence of the antiporter activities between *E. coli* (NhaA) and *Synechocystis* sp. 6803 (SynNHaP) might be interesting to note. It is clearly shown that the point mutations at His-225 of *E. coli* NhaA caused altered responses of the antiporter activity to pH changes. It will be interesting to examine which amino acid residue(s) in the SynNhaP are involved in the constant activity over the wide pH range.

The sequence of 81LFFIYLLPPI90 in TM3 of AtNHX1 is highly conserved with OsNHX1, NHX1, and mammalian NHE (Counillon et al., 1993). In mammals, this region is identified as the binding site of amiloride, which inhibits the eucaryotic Na^+/H^+ exchanger. The sequence of this region in SynNhaP is 68LIMEIFLPPL76 and differs considerably from that of AtNHX1, but is similar to those of SOS1 and NhaP. Because the amiloride sensitivity has only been demonstrated for NHE1 among these antiporters, the relevance of the sequence differences is not clear at this time.

A topological model suggests that the SynNhaP has relatively long C-terminal hydrophilic tail than

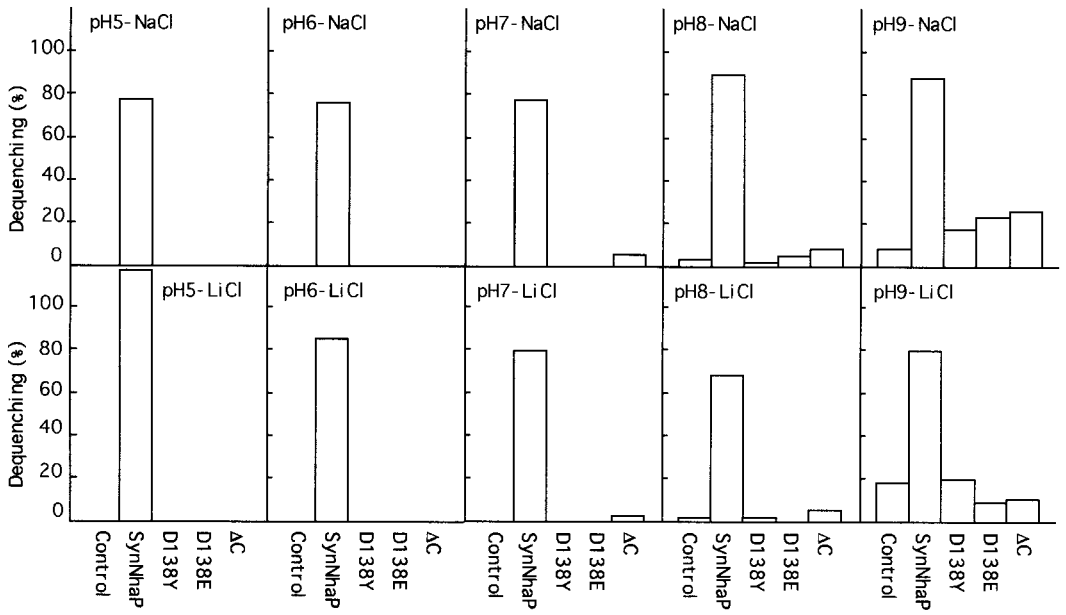

Figure 5. Effects of pH on the Na^+/H^+ and Li^+/H^+ antiporter activity of SynNhaP, SynNhaPD138Y, SynNhaPD138E, and SynNhaPΔC. *E. coli* cells were grown in LBK medium without addition of extra salts. The Na^+/H^+ antiporter activities were measured as described in Figure 4. Each value shows the average of three independent measurements (SE was within 8%).

that of NhaP and *E. coli* antiporters (Fig. 6). In animals, the long C-terminal hydrophilic tails are believed to play a role in the regulation of transport activity (Wakabayashi et al., 1992; Orlowski and Grinstein, 1997). The present results also suggest that the C-terminal hydrophilic tail might interact with the membrane segments and play an important role for the transport activity. Further studies are required to clarify these points.

The recently discovered SOS1 antiporter has been shown to be essential for Na^+ and K^+ homeostatis and its gene expression is up-regulated in response to NaCl stress (Shi et al., 2000). SOS1 was predicted as a 127-kD protein with 12 transmembrane domains in the N-terminal part and a long hydrophilic cytoplasmic tail in the C-terminal part. Since the transmembrane region of SynNhaP and SOS1 has significant sequence similarities, the functional and structural analysis of SynNhaP might also contribute to the understanding of SOS1 antiporter. Construction of the SynNhaP mutants and expression of a large amount of antiporter should help us to study the structural and functional properties of this important protein at the molecular levels.

MATERIALS AND METHODS

Isolation of nhaP Gene

The *nha*P gene from *Synechocystis* sp. 6803 was amplified by PCR using the following primers: forward primer, 5′-CACCATGGATA CAGCGGTCAACG-3′; reverse primer, 5′-TCGAATTCGGATGGTTCGGCCACAT-3′. The forward primer contains the *Nco*I restriction site. The reverse primer contains the *Eco*RI restriction site just before the stop codon. The amplified fragment was ligated into the *Nco*I/*Eco*RI sites of the pTrc-His2C plasmid. The resulting plasmid, pSNhaP, encodes the SynNhaP fused in frame to six histidines, and was used to transform *Escherichia coli* TO114 cells. The DNA sequence was determined using an ABI310 genetic analyzer (PE-Applied Biosystems, Foster City, CA) and analyzed with the DNASIS program (Hitachi Software Engineering, Tokyo).

Construction of SynNhap Mutants

The site-directed mutagenesis of Asp-138 was carried out by using a PCR method (Ito et al., 1991). The 412 to 414 bases, GAT, encoding Asp-138 of SynNhaP were changed to GAA and TAT, which generated the plasmids pSNhaPD138E and pSNhaPD138Y, respectively. The change of nucleotide was confirmed by DNA sequencing. For the construction of C-terminal tail deleted mutant, the pSNhaP plasmid was digested by the restriction enzymes *Pst*I and *Eco*RI, blunted ended, and ligated. The resulting plasmid, pSNhaPΔC, did not contain the last 56 amino acid residues (Leu-472 to Ser-527), but retained the His-tag derived amino acid residues.

Growth of *E. coli* Cells

E. coli TO114 cells, in which *nha*A, *nha*B, and *cha*A were deleted, were used as the host cells. Cells were grown in LBK medium at 37°C under aerobic conditions. The pH of the growth medium was adjusted with KOH or HCl. The growth of cells was monitored by measuring the A_{620} with a Erma AE-22 photoelectric colorimeter.

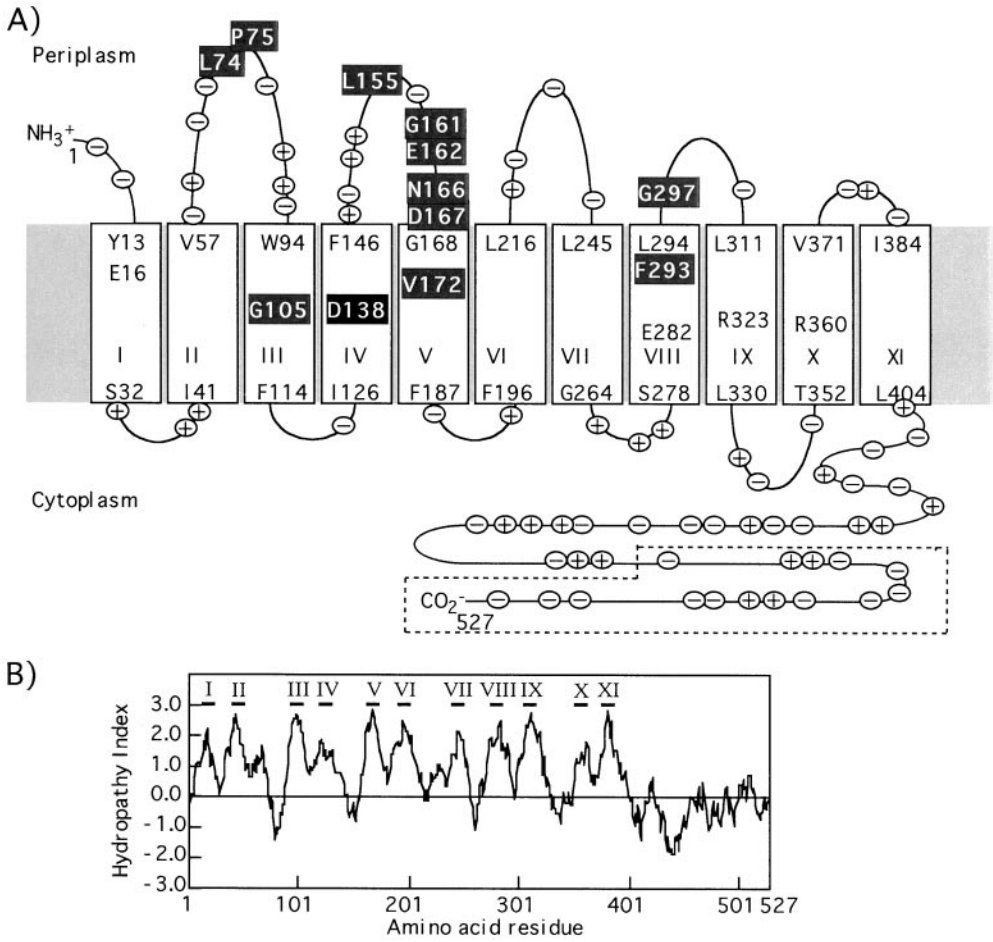

Figure 6. A, Hypothetical secondary structure model of the SynNhaP protein. The possible TMs of the SynNhaP sequence were deduced by a computer program TopPredII. Putative transmembrane helical segments are boxed and the first and the last amino acid of each segment are indicated. Charged amino acids are indicated by + (Arg and Lys) and − (Asp and Glu). The deleted C-terminal tail is boxed by a doted line. B, Hydropathy plot of the SynNhaP protein. Hydropathy values were calculated by the methods of Kyte and Doolittle (1982). The 11 TM segments (I–XI) are indicated by the lines.

Na^+/H^+ Antiporter Activity

The Na^+/H^+ antiporter activity was examined on everted membrane vesicles prepared from the cells grown in LBK as described (Rosen, 1986). *E. coli* cells were harvested by centrifugation at 3,100*g* for 10 min at 4°C and then washed with a suspension buffer TCDS, which contained 10 mM Tris-HCl, pH 7.0, 0.14 M choline chloride, 0.5 mM dithiothreitol, and 0.25 M Suc. The pellets were suspended with 10 mL of TCDS buffer and applied to a French Pressure cell (4,000 psi). Then the solution was centrifuged at 12,000*g* for 10 min at 4°C. The supernatant was centrifuged at 110,000*g* for 60 min at 4°C and suspended in 600 μL of TCDS buffer. The antiporter activity was based upon the establishment of ΔpH (transmembrane pH gradient) by addition of salt to the reaction mixture that contained 10 mM Tris-HCl (titrated with HCl to the indicated pH), 5 mM $MgCl_2$, 0.14 M choline chloride, 1 mM acridine orange, and membrane vesicles (50 μg of protein) in a volume of 2 mL. The ΔpH was monitored at 25°C with acridine orange as a probe at an extinction wavelength of 492 nm (band width 1.5 nm) and emission wavelength of 525 nm (band width 3.0 nm) of Shimadzu RF-5300PC spectrofluorophotometer (Hibino et al., 1995). At the onset of the experiment, Tris-DL-lactate (2 mM) was added and the fluorescence quenching was recorded. Salt (5 mM) was then added and the new steady state of fluorescence obtained (dequenching) after each addition was monitored.

Immunoblotting and Other Methods

SDS-PAGE and immunoblotting were carried out as previously described (Lee et al., 1995; Nomura et al., 1995). Protein was determined by the method of Lowry et al. (1951). An antibody raised against 6-His (6×-His tag) was obtained from R & D Systems (Minneapolis).

Computer Analysis

The hydropathy profile of the deduced amino acid sequence of the SynNhaP was predicted by the computer-assisted procedure according to the method of Kyte and Doolittle (1982). The possible TM of the SynNhaP sequence

was deduced by a computer program TopPredII (Hofmann and Stoffel, 1992).

ACKNOWLEDGMENTS

We greatly appreciate the kind gift of TO114 cells from Dr. H. Kobayashi of Chiba University (Japan). We thank Toshie Inaba and Eiko Tsunekawa (Meijo University, Japan) for their expert technical assistance.

Received July 17, 2000; modified August 28, 2000; accepted September 14, 2000.

LITERATURE CITED

Apse MP, Aharon GS, Snedden WA, Blumwald (1999) Salt tolerance conferred by overexpression of a vacuolar Na^+/H^+ antiport in *Arabidopsis*. Science **285:** 1256–1258

Blumwald E, Cragoe EJ, Poole RJ (1987) Inhibition of Na^+/H^+ antiport activity in sugar beet tonoplast by analogs of amipride. Plant Physiol **85:** 30–33

Counillon L, Franchi A, Pouyssegur J (1993) A point mutation of the Na^+/H^+ exchanger gene (NHE1) and amplification of the mutated allele confer amiloride resistance upon chronic acidosis. Proc Natl Acad Sci USA **90:** 4508–4512

Enomoto H, Unemoto T, Nishibuchi M, Padan E, Nakamura T (1998) Topological study of *Vibrio alginolyticus* NhaB Na^+/H^+ antiporter using gene fusions in *Escherichia coli* cells. Biochim Biophys Acta **1370:** 77–86

Fukuda A, Nakamura A, Tanaka Y (1999) Molecular cloning and expression of the Na^+/H^+ exchanger gene in *Oryza sativa*. Biochim Biophys Acta **1446:** 149–155

Gaxiola RA, Rao R, Sherman A, Grisafi P, Alper SL, Fink GR (1999) The *Arabidopsis thaliana* proton transporters, AtNhx1 and Avp1, can function in cation detoxification in yeast. Proc Natl Acad Sci USA **96:** 1480–1485

Hahnenberger KM, Jia Z, Young PG (1996) Functional expression of the *Schizosaccharomyces pombe* Na^+/H^+ antiporter gene, *sod*2, in *Saccharomyces cerevisiae*. Proc Natl Acad Sci USA **93:** 5031–5036

Hibino T, Lee BH, Rai AK, Ishikawa H, Kojima H, Tawada M, Shimoyama H, Takabe T (1995) Salt enhances photosystem I content and cyclic electron flow via NAD(P) H dehydrogenase in the halotolerant cyanobacterium *Aphanothece halophytica*. Aust J Plant Physiol **23:** 321–330

Hofmann K, Stoffel W (1992) PROFILEGRAPH: an interactive graphical tool for protein sequence analysis. Comput Appl Biosci **8:** 331–337

Inoue H, Noumi T, Tsuchiya T, Kanazawa H (1995) Essential aspartic acid residues, Asp-133, Asp-163 and Asp-164, in the transmembrane helices of a Na^+/H^+ antiporter (NhaA) from *Escherichia coli*. FEBS Lett **363:** 264–268

Ito W, Ishiguro H, Kurosawa Y (1991) A general method for introducing a series of mutations into cloned DNA using the polymerase chain reaction. Gene **102:** 67–70

Jia ZP, McCullough N, Martel R, Hemmingsen S, Young PG (1992) Nucleotide gene amplification at a locus encoding a putative Na^+/H^+ antiporter confers sodium and lithium tolerance in fission yeast. EMBO J **11:** 1631–1640

Kaneko T, Sato S, Kotani H, Tanaka A, Asamizu E, Nakamura Y, Miyajima N, Hirosawa M, Sugiura M, Sasamoto S, Kimura T, Hosouchi T, Matsuno A, Muraki A, Nakazaki N, Naruo K, Okumura S, Shimpo S, Takeuchi C, Wada T, Watanabe A, Yamada M, Yasuda M, Tabata S (1996) Sequence analysis of the genome of the unicellular cyanobacterium *Synechocystis* sp. strain PCC6803: II. Sequence determination of the entire genome and assignment of potential protein-coding regions. DNA Res **3:** 109–136

Kyte J, Doolittle RF (1982) A simple method for displaying the hydropathic character of a protein. J Mol Biol **157:** 105–132

Lee BH, Hibino T, Jo J, Viale AM, Takabe T (1997) Isolation and characterization of *dnaK* genomic locus in a halotolerant cyanobacterium *Aphanothece halophytica*. Plant Mol Biol **35:** 763–775

Lowry OH, Rosebrough NJ, Farr AL, Randall RJ (1951) Protein measurement with the Folin phenol reagent. J Biol Chem **193:** 265–275

Nakamura T, Komano Y, Itaya E, Tsukamoto K, Tsuchiya T, Unemoto T (1994) Cloning and sequencing of an Na^+/H^+ antiporter gene from the marine bacterium *Vibrio alginolyticus*. Biochim Biophys Acta **1190:** 465–468

Nakamura T, Komano Y, Unemoto T (1995) Three aspartic residues in membrane-spanning regions of Na^+/H^+ antiporter from *Vibrio alginolyticus* play a role in the activity of the carrier. Biochim Biophys Acta **1230:** 170–176

Nass R, Cunningham KW, Rao R (1997) Intracellular sequestration of sodium by a novel Na^+/H^+ exchanger in yeast is enhanced by mutations in the plasma membrane H^+-ATPase: insights into mechanisms of sodium tolerance. J Biol Chem **272:** 26145–26152

Nass R, Rao R (1998) Novel localization of a Na^+/H^+ exchanger in a late endosomal compartment of yeast: implications for vacuole biogenesis. J Biol Chem **273:** 21054–21060

Nomura M, Ishitani M, Takabe T, Rai AK, Takabe T (1995) *Synechococcus* sp. PCC7942 transformed with *Escherichia coli bet* genes produces glycine betaine from choline and aquires resistance to salt stress. Plant Physiol **107:** 703–708

Numata M, Petrecca K, Lake N, Orlowski J (1998) Identification of a mitochondrial Na^+/H^+ exchanger. J Biol Chem **273:** 6951–6959

Ohyama T, Igarashi K, Kobayashi H (1994) Physiological role of the *cha*A gene in sodium and calcium circulations at a high pH in *Escherichia coli*. J Bacteriol **176:** 4311–4315

Orlowski J (1993) Heterologous expression and functional properties of amiloride high affinity (NHE-1) and low affinity (NHE-3) isoforms of the rat Na^+/H^+ exchanger. J Biol Chem **268:** 16369–16377

Orlowski J, Grinstein S (1997) Na^+/H^+ exchangers of mammalian cells. J Biol Chem **272:** 22373–22376

Padan E, Schuldiner S (1996) Bacterial Na^+/H^+ antiporters: molecular biology, biochemistry, and physiology. *In* WN Konings, HR Kaback, JS Lolkema, eds, Handbook of Biological Physics, Vol 2. Elsevier Science, Amsterdam, pp 501–531

Pinner E, Padan E, Schuldiner S (1995) Amiloride and harmaline are potent inhibitors of NhaB, a Na^+/H^+ antiporter from *Escherichia coli*. FEBS Lett **365:** 18–22

Rosen BP (1986) Ion extrusion systems in *Escherichia coli*. Methods Enzymol **125:** 328–336

Sardet C, Franchi A, Pouyssegur J (1989) Molecular cloning, primary structure, and expression of the human growth factor-activatable Na^+/H^+ antiporter. Cell **56:** 271–280

Shi H, Ishitani M, Kim C, Zhu JK (2000) The *Arabidopsis thaliana* salt tolerance gene SOS1 encodes a putative Na^+/H^+ antiporter. Proc Natl Acad Sci USA **97:** 6896–6901

Utsugi J, Inaba K, Kuroda T, Tsuda M, Tsuchiya T (1998) Cloning and sequencing of a novel Na^+/H^+ antiporter gene from *Pseudomonas aeruginosa*. Biochim Biophys Acta **1398:** 330–334

von Heijne G, Gavel Y (1988) Topogenic signals in integral membrane proteins. Eur J Biochem **174:** 671–678

Wakabayashi S, Fafournoux P, Sardet C, Pouyssegur J (1992) The Na^+/H^+ antiporter cytoplasmic domain mediates growth factor signals and controls "$H(^+)$-sensing." Proc Natl Acad Sci USA **89:** 2424–2428

Wakabayashi S, Pang T, Su X, Shigekawa M (2000) A novel topological model of the human Na^+/H^+ exchanger isoform 1. J Biol Chem **275:** 7942–7949